

N. MATTIUCCI^{1,2,3}
G. D'AGUANNO^{1,2}, ✉
M. SCALORA²
M. J. BLOEMER²

Cross-phase modulation in one-dimensional photonic crystals: applications to all-optical devices

¹Time Domain Corporation, Cummings Research Park, 7097 Old Madison Pike, Huntsville, AL 35806, USA
²Charles M. Bowden Research Center, RDECOM Bldg 7804, Redstone Arsenal, AL 35898-5000, USA
³Università 'RomaTre', Dipartimento di Fisica 'E. Amaldi', Via Della Vasca Navale 84, 00146 Rome, Italy

Received: 16 March 2005

Published online: 2 June 2005 • © Springer-Verlag 2005

ABSTRACT We present a numerical study of a finite photonic band gap structure with a $\chi^{(3)}$ nonlinearity that couples two input pump beams at frequencies ω_1 and ω_2 . We show that in this configuration a variety of all-optical devices can be obtained: an optical transistor, a double switch, and a dynamical switch.

PACS 42.65.-k; 42.65.Pc; 42.79.-e

1 Introduction

The seminal work of Chen and Mills [1] on the appearance of gap solitons in one-dimensional photonic crystals (1-D PCs) with a $\chi^{(3)}$ nonlinearity can be characterized as the beginning of a period of intense experimental and theoretical investigations whose focus was to study the possibility of using these structures as all-optical devices: as switching and limiting devices, and as diodes [2–8]. Although a large number of papers have already been published on the subject, the vast majority of them generally consider configurations with only one input pump beam, limiting the flexibility of the proposed devices. In Ref. [8] a more flexible configuration was studied, but the proposed device is an electro-optic rather than an all-optical device. Here we study an all-optical device based on a two-pump scheme, where the two pumps are coupled by the cross phase modulation terms of the cubic nonlinearity. In particular, we will discuss an optical transistor, a double switch, and a dynamical switch. The paper is organized as follows: in Sect. 2 we briefly discuss the mathematical model and the characteristics of the PC structure used for the simulations; Sect. 3 is devoted to the optical transistor and the double switch; finally in Sect. 4 we study the dynamical switch.

2 The model

Our study is based on the plane monochromatic wave approach. Two input beams, of frequencies ω_1 and ω_2 ,

respectively, propagate in the z direction and arrive at normal incidence at the input surface of a 1-D PC composed of alternating layers of a linear dielectric material juxtaposed to a nonlinear dielectric material with a cubic nonlinearity. The two waves are assumed to be linearly polarized in the same direction. The problem can be described by the following system of nonlinear coupled differential equations:

$$\begin{cases} \frac{d^2 E_1}{dz^2} + \frac{\omega_1^2}{c^2} [n_1(z) + 3\sigma_{11}(z)|E_1|^2 + 6\sigma_{21}(z)|E_2|^2] \\ \quad \times E_1 = 0, \\ \frac{d^2 E_2}{dz^2} + \frac{\omega_2^2}{c^2} [n_2(z) + 3\sigma_{22}(z)|E_2|^2 + 6\sigma_{12}(z)|E_1|^2] \\ \quad \times E_2 = 0, \end{cases} \quad (1)$$

where E_1 and E_2 are the amplitudes of the electric fields, normalized with respect to the input amplitudes, at frequencies ω_1 and ω_2 , respectively. The dimensionless coefficients σ are the elements of the $\chi^{(3)}$ tensor multiplied by the square modulus of the related input amplitudes (i.e. $\sigma_i(\omega_j) = \chi^{(3)}(\omega_i, \omega_i, \omega_j)|E_i^{(0)}|^2$). For simplicity, we assume that the $\chi^{(3)}$ tensor is not dispersive, so that $\sigma_{11} = \sigma_{12} = \sigma_1$ and $\sigma_{21} = \sigma_{22} = \sigma_2$. n_1 and n_2 are the z -dependent, linear refractive indices, at frequencies ω_1 and ω_2 , respectively. We consider a 1-D PC composed of $N = 40$ periods, and we assume that the elementary cell is made of two layers of non-dispersive and non-absorbing dielectric materials of low refractive index $n_L = 1.7$, $\lambda/4n_L$ thick, and high refractive index $n_H = 3.5$, $\lambda/2n_H$ thick, respectively. The reference wavelength is $\lambda = 1 \mu\text{m}$. The low-index layer exhibits the $\chi^{(3)}$ nonlinearity.

In Fig. 1 we show the linear transmission (T) of the structure. The arrows indicate the tuning of the two incident pumps. The ω_1 pump is tuned at the low frequency band edge transmission resonance, while the ω_2 pump is tuned at the high frequency band edge transmission resonance. In both cases $T \sim 1$. We note that this structure was not optimized for the devices that will be studied in the next sections. So, we seek proof-of-principle results and an understanding of the qualitative aspects of the dynamics that ensues when two pumps are coupled as in Eq. (1) above. Moreover, although in our calculations we use a $\lambda/4-\lambda/2$ structure, similar results can be expected for different types of structures. We numerically

✉ Fax: +1-256-9557216, E-mail: giuseppe.daguanno@timedomain.com

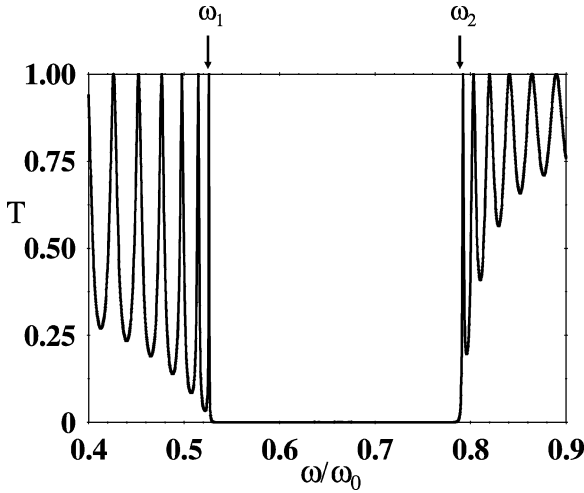


FIGURE 1 Linear transmission vs. ω/ω_0 , where $\lambda_0 = 1 \mu\text{m}$ is the reference wavelength and $\omega_0 = 2\pi c/\lambda_0$. The structure is composed of $N = 40$ periods. The elementary cell consists of two layers of refractive indices $n_H = 3.5$ and $n_L = 1.7$, respectively. The thicknesses of the two layers are respectively $d_H = \lambda_0/2n_H$ and $d_L = \lambda_0/4n_L$. The structure is surrounded by air ($n_0 = 1$). The arrows indicate the positions of the two pumps (ω_1 and ω_2) on the transmission spectrum

integrate Eq. (1) using a shooting procedure, as described in Refs. [9, 10], for example.

3 Optical transistor and double switch

In electronics, a transistor is made of three layers of a doped semiconductor material. The three-layer structure consists of an n-type (p-type) semiconductor layer sandwiched between two p-type (n-type) layers. In such a device a small change in the current or voltage at the inner semiconductor layer, which acts as control, produces a large change in the current passing through the entire structure. The device can thus act as a switch, opening and closing an electronic gate. From this point of view, the optical configuration we propose shows transistor-like behavior. In Fig. 2 we show that a small change in the intensity of the ω_2 pump produces a large change in the transmitted intensity of the ω_1 field (dashed line), a behavior that is due to the optical bistability induced by the ω_2 pump. In fact, if we turn off the electric field E_2 and allow the intensity of the ω_1 pump to vary, no bistable behavior is noted (Fig. 2, solid line). The ω_2 pump also manifests bistable behavior, as shown in Fig. 3. The device can then be used as a double switch, as the switching point of the transmitted fields at ω_1 and ω_2 is the same for both curves. In Figs. 4 and 5 we show the square moduli of E_1 and E_2 , respectively, inside the PC before the switch (thin solid line), when $\sigma_1 = 0.002$ and $\sigma_2 = 0.002$, and after the switch (thick solid line), when $\sigma_1 = 0.002$ and $\sigma_2 = 0.03$. Note that for $\sigma_1 = 0.002$ the nonlinear transmission for ω_1 is $T \sim 0.75$, and E_1 has the characteristic bell-shaped envelope consistent with its tuning very near the peak of transmission of the low frequency band edge [11], close to its original tuning position. This clearly indicates that the transmission resonance for the ω_1 pump has suffered a small, nonlinear shift toward low frequencies. On the other hand, for the same control parameter (i.e. $\sigma_2 = \sigma_1 = 0.002$), the high frequency band edge transmission resonance has already suffered a large

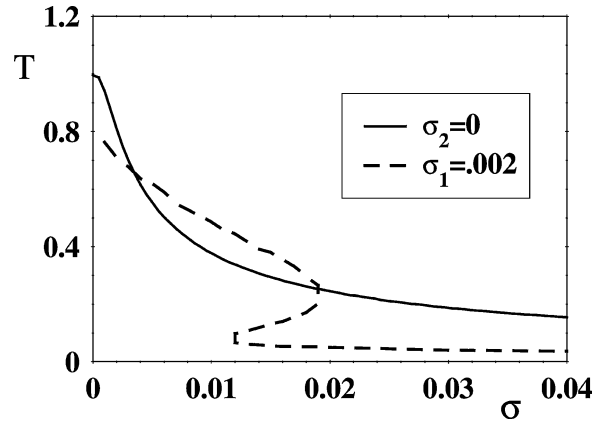


FIGURE 2 Nonlinear transmission of the electric field E_1 . The solid line is the transmission of the electric field E_1 as a function of its own control parameter $\sigma_1 = \chi^{(3)}|E_1^{(0)}|^2$ (the second pump ω_2 is in this case turned off: i.e. $\sigma_2 = 0$). $E_j^{(0)}$, with $j = 1, 2$, are the amplitudes of the input fields at frequencies ω_1 and ω_2 , respectively. The dashed line is the transmission of the electric field E_1 as a function of the control parameter $\sigma_2 = \chi^{(3)}|E_2^{(0)}|^2$ (the first pump ω_1 is in this case set at a fixed value: $\sigma_1 = 0.002$). In the first case (solid line) in the abscissa axis σ stays for σ_1 while in the second case (dashed line) σ stays for σ_2

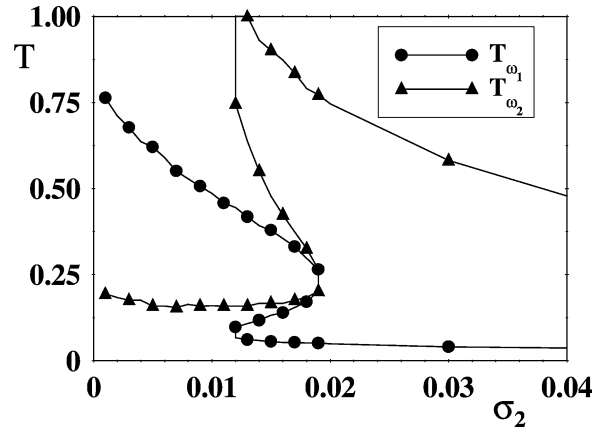


FIGURE 3 Transmission of the electric fields E_1 and E_2 vs. σ_2 . The control parameter of the first pump is set at $\sigma_1 = 0.002$

shift toward low frequencies causing the E_2 field to ‘fall’ in the valley between the first and the second transmission resonances, at the high-frequency band edge, with $T \sim 0.25$. The different behavior of the two fields can be easily explained because of their different localization properties within the PC: E_1 is initially mostly localized in the linear, high-index layers, while E_2 is initially localized in the nonlinear, low-index, layers. After switching occurs, the nonlinear shift of the transmission causes the E_1 field to fall inside the gap, near the low-frequency band edge. The E_2 field is then tuned near the second peak of transmission of the high-frequency band edge, consistent with its double-bell-shaped envelope.

4 Dynamical switch

A simple all-optical switch in PC structures with a cubic nonlinearity has been studied in Refs. [3, 4]. In the present case, our device can benefit from additional flexibility by dynamically (or parametrically) controlling the switching

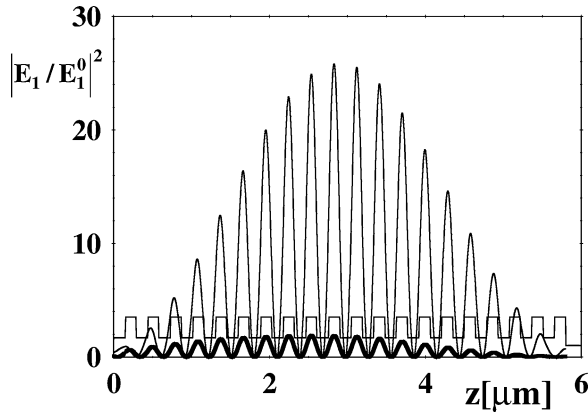


FIGURE 4 Square modulus of $E_1/E_1^{(0)}$ inside the structure. The *thick solid line* represents the field profile after the switching ($\sigma_1 = 0.002$ and $\sigma_2 = 0.03$). The *thin solid line* represents the field profile before the switching ($\sigma_1 = 0.002$ and $\sigma_2 = 0.002$)

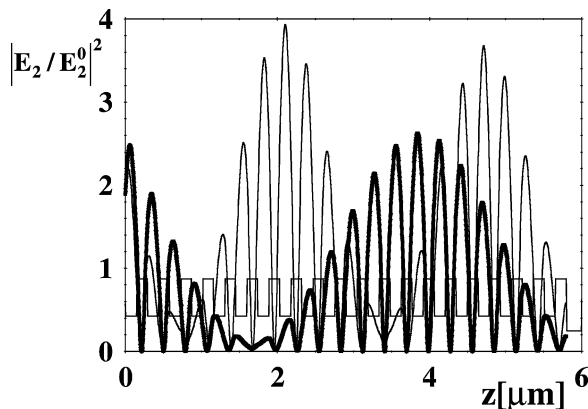


FIGURE 5 Square modulus of $E_2/E_2^{(0)}$ inside the structure after the switching (*thick solid line*) for $\sigma_1 = 0.002$ and $\sigma_2 = 0.03$ and before the switching (*thin solid line*) for $\sigma_1 = 0.002$ and $\sigma_2 = 0.002$

point of the E_2 field using the intensity of the E_1 field. In other words, we fix the intensity of the E_1 input field, vary the intensity of the E_2 field, and so monitor the change of the switching point of the E_2 field for different values of the E_1 intensity. In Fig. 6 we calculate the nonlinear transmission curves of the E_2 field vs. σ_2 for different values

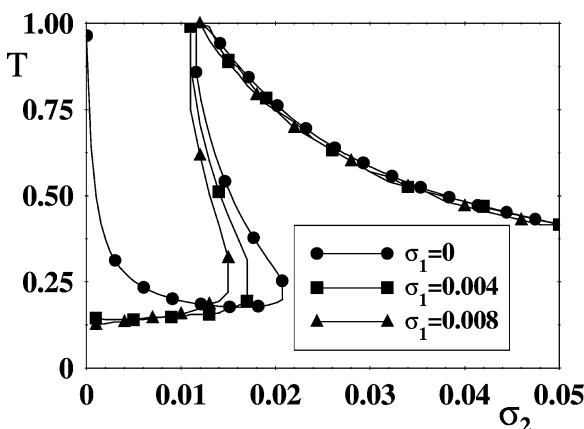


FIGURE 6 Transmission of the electric field E_2 vs. σ_2 for different values of the control parameter σ_1

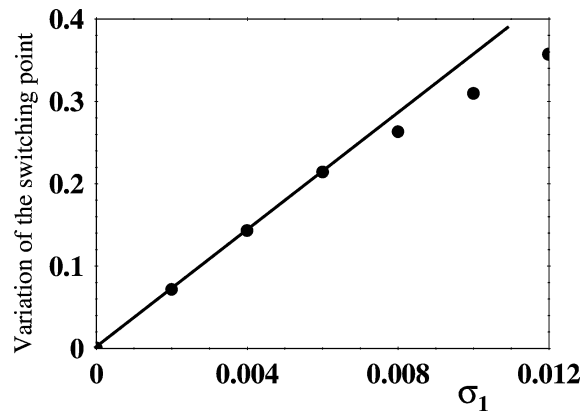


FIGURE 7 Variation of the switching point of the E_2 field vs. σ_1 . The switching point is indicated as σ_{2s} and the relative variation of the switching point is calculated as follows: $(\sigma_{2s}(\sigma_1 = 0) - \sigma_{2s}(\sigma_1)) / \sigma_{2s}(\sigma_1 = 0)$. The *circles* represent the actual calculated data. The *straight, solid line* connecting the first points indicates that the variation of the switching point is linear only for small values of the control parameter σ_1 . In this case saturation effects come into play above $\sigma_1 \sim 0.006$

of the parameter σ_1 ($\sigma_1 = 0; 0.004; 0.008$). The figure shows that the switching point is reached for lower values of σ_2 as σ_1 increases. In other words, the larger the intensity of the ω_x pump, the lower the intensity of the ω_2 pump will be to achieve self-switching. In Fig. 7 we show the variation of the switching point (σ_{2s}) as a function of the σ_1 parameter. Note that while for low values of σ_1 the curve is linear, for higher values of σ_1 the curve show saturating behavior.

5 Conclusions

In summary, we have shown that a 1-D PC doped with a $\chi^{(3)}$ nonlinearity, and pumped with two electromagnetic fields, can act as a more versatile device compared to having just a single pump. The switching properties of the structure [3, 4, 7] can be improved by using a double-pumping scheme such that both pumps are tuned to their respective band edges, and become localized inside the stack. The dynamics that ensues gives rise to a double switch (Fig. 3) and to a dynamical switch (Fig. 6). An all-optical transistor (Fig. 2) is also envisioned.

REFERENCES

- 1 W. Chen, D.L. Mills, Phys. Rev. Lett. **58**, 160 (1987)
- 2 J. He, M. Cada, Appl. Phys. Lett. **61**, 2150 (1992)
- 3 B. Acklin, M. Cada, J. He, M.-A. Dupertuis, Appl. Phys. Lett. **63**, 2177 (1993)
- 4 M. Scalora, J.P. Dowling, C.M. Bowden, M.J. Bloemer, Phys. Rev. Lett. **73**, 1368 (1994)
- 5 M. Scalora, J.P. Dowling, C.M. Bowden, M.J. Bloemer, J. Appl. Phys. **76**, 2023 (1994)
- 6 M.D. Tocci, M.J. Bloemer, M. Scalora, J.P. Dowling, C.M. Bowden, Appl. Phys. Lett. **66**, 2324 (1995)
- 7 S. Janz, J. He, Z.R. Wasilewski, M. Cada, Appl. Phys. Lett. **67**, 1051 (1995)
- 8 P. Xie, Z.-Q. Zhang, J. Appl. Phys. **95**, 1630 (2004)
- 9 R.S. Bennink, Y.-K. Yoon, R.W. Boyd, J.E. Sipe, Opt. Lett. **24**, 1416 (1999)
- 10 W.H. Press, B.P. Flannery, S.A. Teukolsky, W.T. Vetterling, *Numerical Recipes in C* (Cambridge University Press, Cambridge, 1988)
- 11 G. D'Aguanno, M. Centini, M. Scalora, C. Sibilia, Y. Dumeige, P. Vidakovic, J.A. Levenson, M.J. Bloemer, C.M. Bowden, J.W. Haus, M. Bertolotti, Phys. Rev. E **64**, 16 609 (2001)